International Journal of the Korean Society of Precision Engineering Vol. 3, No. 4, October 2002.

Dynamic System Analysis of Machine Tool Spindles with Magnet Coupling

Seong Keol Kim

Graduate School of Automotive Engineering, Kookmin University, Seoul, Korea

ABSTRACT

In this study, basic concepts of magnet were introduced, and dynamic characteristics of magnet coupling were explored. Based on these characteristics, it was proposed how to analyze transverse and torsional vibrations of a spindle system with magnet coupling. Proposed theoretical approaches were applied to a precision power transmission system machined for this study, and the transverse and torsional vibrations were simulated. The force on magnet coupling was shown as a form of nonlinear function of the gap and the eccentricity. Also, the form of torque transmitted by magnet coupling was considered as a sinusoidal function. Main spindle connected to a coupling of a follower part was assumed to be a rigid body. Nonlinear partial differential equation was derived to be as a function of angular displacement. By using the equation, torsional vibration analysis of a spindle system with magnet coupling was performed. Free and forced vibration analyses of a spindle system with magnetic coupling were explored by using FEM.

Keywords : Precision power transmission system, Magnet coupling, Nonlinear spring, Nonlinear partial differential equation, Torsional vibration, Transverse vibration, Angular displacement, Gap, Eccentricity

1. Introduction

The driving system in precision machine tool to machine precision parts should be designed to be high dynamic performance. Generally, the role of power transmission device, especially coupling is to connect motor to main spindle without power loss and etc. In couplings, there are two types, the contact way and the non-contact way. The second shows a better isolation of vibration than the first. Magnet coupling is a sort of non-contact power transmission devices, and transmits torque by magnetic force.

Studies relating to materials and mechanical properties of permanent magnet had made successful results in late 1,970s, and among them, studies on characteristics of magnet coupling and magnetic bearing have been performed by C.J.Fellow [1], J.P.Yonnet [2], [3] and etc. Motivation of this research is why previous studies were confined to only dynamic characteristics of magnet coupling itself, and dynamic analysis of a spindle system with magnet coupling has been few. However a lot of studies relating to coupling itself have been performed, especially, by domestic researchers [11]~[14].

From this motivation, researches have tried to be like; the first, the relation [1] of transmitted torque and relative angular displacement between a driver and a follower is explored, the second, transmitted forces and equivalent stiffnesses of axial and radial directions are studied in existence of eccentricity, the third, in order to analyze torsional vibration due to non-uniform angular velocity of a driver, a spindle system connected to magnet coupling of a follower part is modeled as a rigid body, and responses of a main spindle by applying harmonic excitation to a coupling of a driver part are obtained, the forth, longitudinal vibration due to eccentricity is explored, last, by modeling a spindle system with magnet coupling in FEM, free vibration analyses for changing the gap and the type of couplings are performed, and also forced vibrations are analyzed to explore the effects of vibration isolation by using magnet coupling when harmonic excitation is applied to a coupling of a driver part.

2. Consideration of dynamic characteristics of magnet coupling

2.1 Relation of transmission torque and angular displacement between couplings

Couplings used in this study are synchronous couplings to transmit torque between two magnets with existence of constant gap in two permanent magnets. Transmission torque has no relation with rotation velocity of a spindle, and depends on relative angular displacements of magnets attached to couplings of a driver and a follower. Also, the magnets move with synchronous velocities. In synchronous couplings, there are two types, axial (CR model), and face (CD model).

The relation of the torque transmitted by synchronous permanent magnet coupling and the angular displacements was proposed by Fellows [1], Weissmann [7] and etc. It is like equation (1), and shown in Fig. 1.

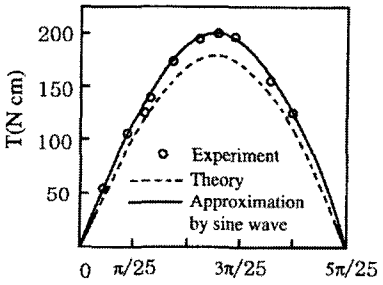

Fig. 1 Experimental and theoretical results of transmission torque of magnet coupling by Weissmann et al.

$$T = T_m \sin \varphi_m \tag{1}$$

,where φ_m is angle between a driver and a follower

2.2 Relations of transmission force, axial stiffness and eccentricity

In view of linear displacement analysis of a spindle in existence of eccentricity, Park [8] showed the results of the explorations for magnet speed and working force variations. In this study, simulations for axial and radial forces due to eccentricity between a driver and a follower are performed. Magnetic field, H for a bar-shaped magnet is like equation (2), and geometrical configuration of magnets is shown in Fig. 2.

$$H_1 = \int_{S_1} dH_1 \tag{2}$$

,where,

$$dH_1 = \begin{Bmatrix} dH_{r_1} = \dfrac{1}{2\pi\mu_0} J_1 dS_1 \dfrac{\cos(\theta - \beta_1)}{r_{12}^2} \\ dH_{\theta_1} = \dfrac{1}{2\pi\mu_0} J_1 dS_1 \dfrac{\sin(\theta - \beta_1)}{r_{12}^2} \end{Bmatrix}$$

,where J_1 is magnetization, and S_1 is cross sectional area of magnet

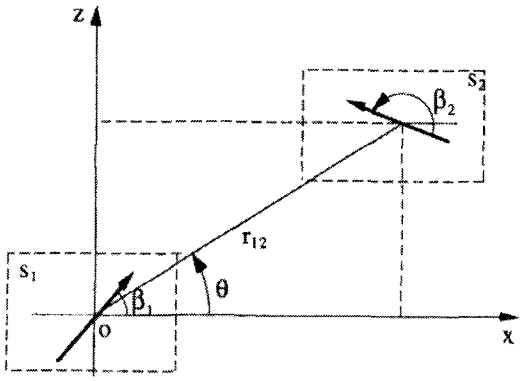

Fig. 2 A geometrical configuration of magnets

Internal energy to exist at magnetic field by the 1st magnet is shown like equation (3).

$$\begin{aligned} dW &= -J_2 H_1 dv_2 \\ J_2 &= \begin{Bmatrix} H_{2_r} = J_2 \cos(\beta_3 - \theta) \\ H_{2_\theta} = J_2 \sin(\beta_3 - \theta) \end{Bmatrix} \\ dv_2 &= dS_2 dl \end{aligned} \tag{3}$$

Therefore, magnetic e nergy p er unit l ength b y t wo magnets is equation (4).

$$\frac{W}{l} = \int_{S_1}\int_{S_2} \frac{1}{2\pi\mu_0} \frac{J_1 J_2}{r_{12}^2} \cos(\beta_1 + \beta_2 - 2\theta) dS_1 dS_2 \tag{4}$$

where l is length of magnet.

Equation (4) is differentiated to obtain x and z-direction forces, F_x and F_z.

$$\begin{aligned} \frac{F_x}{l} &= \frac{dW}{dx} = -\left(\frac{\partial W}{\partial r_{12}} \cdot \frac{\partial r_{12}}{\partial x} + \frac{\partial W}{\partial \theta} \cdot \frac{\partial \theta}{\partial x} \right) \\ &= \int_{S_1}\int_{S_2} \frac{-1}{\pi\mu_0} \frac{J_1 J_2}{r_{12}^3} \cos(\beta_1 + \beta_2 - 3\theta) dS_1 dS_2 \end{aligned} \tag{5}$$

$$\frac{F_z}{l} = \frac{dW}{dz} = -\left(\frac{\partial W}{\partial r_{12}} \cdot \frac{\partial r_{12}}{\partial z} + \frac{\partial W}{\partial \theta} \cdot \frac{\partial \theta}{\partial z}\right)$$
$$= \int_{S_1}\int_{S_2} \frac{1}{\pi\mu_0} \frac{J_1 J_2}{r_{12}^3} \sin(\beta_1 + \beta_2 - 3\theta) dS_1 dS_2 \quad (6)$$

where

$$r_{12} = \sqrt{x^2 + z^2},\ \tan\theta = \frac{z}{x}$$

Relations of the forces working on magnet and the equivalent stiffnesses are like equation (7).

$$K_x = -\frac{dF_x}{dx},\quad K_z = -\frac{dF_z}{dz} \quad (7)$$

And, axial equivalent stiffness, K_z can be shown like equation (8).

$$\frac{K_z}{l} = \int_{S_1}\int_{S_2} \frac{3}{\pi\mu_0} \frac{J_1 J_2}{r_{12}^4} \cdot \cos(\beta_1 + \beta_2 - 4\theta) dS_1 dS_2 \quad (8)$$

In face-typed magnet coupling, relation of axial and radial equivalent stiffnesses is as follows;

$$K_r = -\frac{K_z}{2} \quad (9)$$

For face-typed magnet coupling by using above equations, relation of axial equivalent stiffness and eccentricity is shown in Fig. 3.

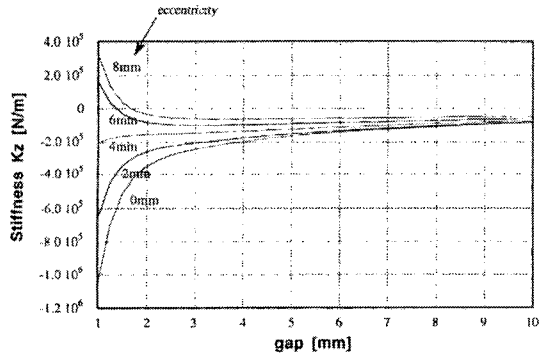

Fig. 3 Relation of axial equivalent stiffness (K_z) and eccentricity by changing gap for face typed magnet coupling, model CD85F

In above results, negative values of stiffness mean what restoring force is working, and its positive values are what repulsive force is working. In case that eccentricity is over 6 mm, the system becomes unstable as shown in Fig. 3. Since it is almost never happened that the eccentricity is over 1 mm in real operating condition of machine tools, instability due to eccentricity is not a problem.

3. Torsional vibration[4), (5)]

3.1 Theory

A rotating spindle system with magnet coupling is shown in Fig. 4.

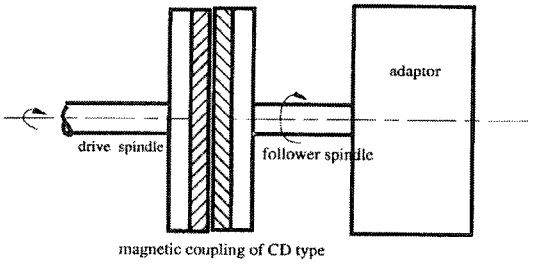

Fig. 4 A schematic of rotating spindle with magnet coupling

In order to analyze torsional vibration of a spindle system with magnet coupling, a mathematical model was built like Fig. 5.

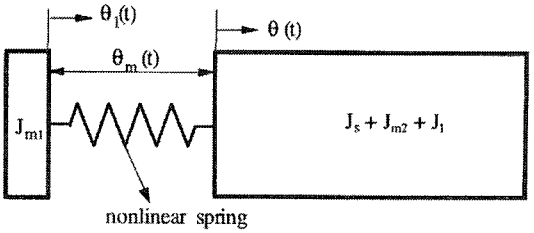

Fig. 5 A mathematical model of rotating spindle with magnet coupling

θ_i : applied angular displacement
θ : angular displacement of response
J_{m1} : polar mass moment of inertia for magnet coupling of a driver part
J_{m2} : polar mass moment of inertia for magnet coupling of a follower part
J_s : polar mass moment of inertia for main spindle
J_a : polar mass moment of inertia for adaptor

Torque transmitting between couplings can be shown as a sinusoidal function of relative angle of a driver and a follower, θ_m[6-7]. This torque was modeled as a nonlinear spring, and a governing equation was derived like equation (10).

$$(J_{m2} + J_s + J_a)\frac{d^2\theta}{dt^2} = T_m \sin(\theta_1 - \theta) \tag{10}$$

,where

$$J_T = J_{m2} + J_s + J_a$$
$$\theta_m = \theta - \theta_1$$

In torsional vibration analysis, angle of input excitation, θ_1 assumed to be a sinusoidal function like equation (11), and from equation (10), equation (12) was built.

$$\theta_1 = A\cos\omega t \tag{11}$$

A : amplitude of excitation

ω : excitation frequency

$$\frac{d^2\theta_m}{dt^2} + \omega_n^2 \sin\theta_m = \omega^2 A\cos\omega t$$
$$\omega_n^2 = T_m / J_T \tag{12}$$

Taylor expansion series of θ_m like equation (13) was used, and from equations (12) and (13), finally equation of motion was built.

$$\sin\theta_m = \theta_m - \frac{\theta_m^3}{6} \tag{13}$$

$$\frac{d^2\theta_m}{dt^2} + \omega_n^2\left(\theta_m - \frac{\theta_m^3}{6}\right) = \omega^2 A\cos\omega t \tag{14}$$

Equation (14) has the similar shape of Duffing equation. By using Ritz's averaging method, θ_m is assumed to be equation (15), and from equations (14) and (15), relation of amplitude and frequency ratio is equation (16).

$$\theta_m = a\phi(t) = a\cos\omega t \tag{15}$$

a : weight factor(amplitude of response)

$\phi(t)$: selected time function

$$\frac{1}{8}a^3 = a\left[1 - \left(\frac{\omega}{\omega^2}\right)^2\right] - \left(\frac{\omega}{\omega^2}\right)^2 A \tag{16}$$

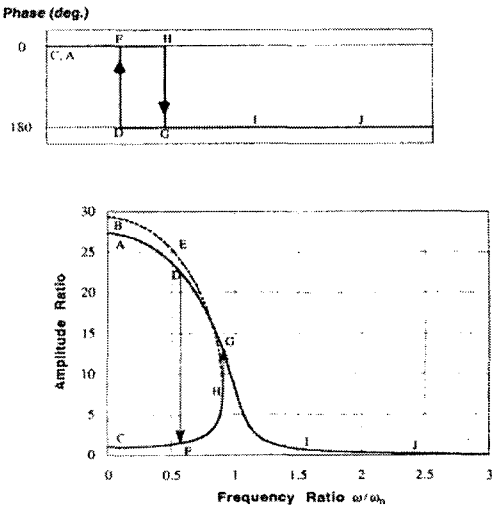

Fig. 6 Simulation of torsional vibration of a spindle with magnet coupling for changing frequency ratio

3.2 Results of simulations

When amplitude of excitation, A is given to be 0.1 radian, amplitude variations of angular displacement at a coupling of a follower part are shown in Fig. 6 for frequency ratio.

As excitation frequency increases at ω/ω_n = 0, amplitude also increase along CFH as shown in Fig. 6, and jump-up phenomenon is shown from point H to G. At range of higher frequency ratio, amplitude goes along GIJ, and converges to be a zero. As excitation frequency decreases at much larger level than ω_{cr}, amplitude changes along JIGDFC as shown in Fig. 6, and jump-down is shown from D to F. Range, HEB is unstable, and is not happened at test. Point H is shown at ω_{cr}, and ω_{cr}/ω_n is 0.90633.

4. Transverse vibration

4.1 Theory

A precision power transmission system to explore transverse vibration is shown in Fig. 7.

In this system, sub-spindle is supported by two types of ball bearings, and main spindle is supported by air bearing. For FEM modeling of a spindle system, first, equivalent stiffnesses of two types of ball bearings should be known. Stiffness of ball bearing supporting sub-spindle has nonliearity, and generally is given as a experimental equation [9], [10].

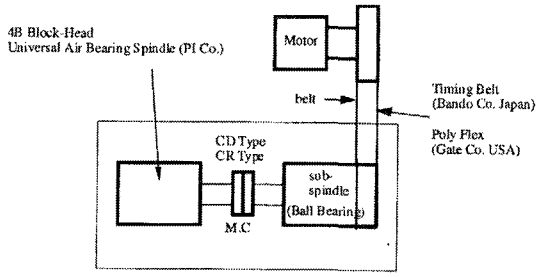

Fig. 7 A schematic of a precision power transmission system

$$k_{eq} = \frac{dF_r}{dS} = \frac{n}{\zeta} ZK\delta^{n-1}\cos\alpha \qquad (17)$$

Z : number of balls

δ : deflection

n : constant(1.5 for ball bearing)

α : contact angle

K : load-deflection constant

ζ : constant

Equivalent stiffness of air bearing supporting main spindle is changed by air pressure and etc. Air pressure of 4" Block-Head Universal air bearing spindle of PI(USA) used at test is 150psi, and each stiffness is as follows;

Axial stiffness : 35.72 kgf/μm

Radial stiffness : 11.91 kgf/μm

Angular stiffness : 4.61×10^{-2} kbf m/μrad

By using above values, each bearing was modeled as a truss element of equivalent stiffness. Since sub-spindle and main spindle were modeled as a beam element, torsional vibration was ignored and bending was only considered. Also, permanent magnet coupling part and adaptor were modeled as a beam element. As the results of FEM, deflections of these parts were not almost shown like a rigid body motion. This was why their stiffnesses were much larger than that of spindle. Loads and equivalent stiffnesses working between a driver and a follower in coupling were obtained by equations (3)~(9).

4.2 Results of FEM simulations

4.2.1 Free vibration

FEM modeling for a precision power transmission system was built by using SUPER-SAP commercial program, and free vibration simulations were performed for 3 types of magnet couplings (face type, CD model). The results are given in Table 1.

Table 1 Results of free vibration of the system by using FEM at gap = 3 mm

Mode	Natural frequencies (Hz)		
	CD 50F	CD 85F	CD 100F
1	522	458	429
2	545	476	446
3	661	657	656
4	789	788	786
5	914	915	913
6	917	916	914
7	970	1158	1190
8	993	1179	1212
9	2130	2084	2058
10	2131	2085	2060

As shown in Table 1, natural frequencies of the system were changed by type of magnet coupling. Generally, larger coupling means increase of equivalent stiffness. However, since increasing quantity of mass is relatively larger than that of stiffness in CD typed magnet coupling, natural frequencies are shown to be smaller as magnet coupling are larger.

4.2.2 Forced vibration

Forced vibration was performed also by FEM to explore the effect of vibration isolation by magnet coupling. The same FEM model used in free vibration analysis was also used, and 100 N external dynamic force was applied to sub-spindle as a sinusoidal function. The ratio of the deflection (input) of excitation part (sub-spindle) and maximum dynamic displacement (output) of right side of a main spindle was calculated, and it was output/input. The magnet coupling was equipped between a sub-spindle and a main spindle as shown in Fig. 7. The results of simulation are shown in Table 2.

Through the simulations, results and discussions are as follows, first, as rotating speed of motor increases, deflections of excitation part decrease, and also dynamic displacements of right side of a main spindle decrease. The second, larger effect of vibration isolation at gap = 5 mm than gap = 3 mm between a driver and a follower in

coupling is given in all simulations. This is why equivalent stiffness is a nonlinear function of gap, and is more flexible at larger gap. The third, smaller sized coupling is shown to be better vibration isolation since equivalent stiffness of CD 50F is more flexible than that of CD 100F as shown in the results of transverse displacement analysis. Theoretically, more flexible equivalent stiffness in non-contact typed coupling makes larger effect of vibration isolation, however large sized coupling is needed to transmit dynamic power of a driver to that of a main spindle, a follower precisely. The forth, through these simulations, vibration isolation by magnet coupling can be shown large effect.

Table 2 Results of forced vibration simulations in a spindle system with magnet coupling (ratio)

Excitation frequency	Gap (mm)	Type of magnet coupling		
		CD 100F	CD 85F	CD 50F
500 rpm	3	0.0830	0.0809	0.0677
	5	0.0802	0.0780	0.0576
1,000 rpm	3	0.0798	0.0783	0.0664
	5	0.0769	0.0752	0.0562
1,500 rpm	3	0.0815	0.0792	0.0654
	5	0.0789	0.0762	0.0558

5. Conclusions

In this study, basic concepts of magnet were introduced, and dynamic characteristics of magnet coupling were explored. Based on these characteristics, it was proposed how to analyze transverse and torsional vibrations of a spindle system with magnet coupling. Proposed theoretical approaches were applied to a precision power transmission system machined for this study, and the transverse and torsional vibrations were simulated.

More detailed results and discussions are shown as follows; the first, since permanent magnet itself has instability of material, magnet coupling should produce the ability at unstable state. Such instability can be known through severely decreasing trend of stiffness at smaller gap between couplings. The second, in simulations of transverse vibration, equivalent stiffness was obtained for some types of magnet coupling. In case that gap was over 3 mm, stability was being kept, and it was possible to transmit dynamic power. Also, stability of the system could be kept from aligning centers of a driver and a follower without eccentricity. The third, through simulations of torsional vibration, it was found that torsional vibration of a main spindle did not almost produce in case that excitation frequency was over twice of natural frequency of the system, and phase difference between couplings of a driver and a follower was 180°. The forth, through simulations of transverse vibration of a main spindle system with CD typed magnet coupling, it was found that the 1st natural frequency was larger than 400 Hz. Since this frequency is much larger than 1,500~2000 rpm, which is general operating speed in machine tools, resonance never happens in these operating speed ranges. Last, through simulations of forced vibration of a spindle system, it was found that the deflection at a main spindle was much smaller than that at excitation part. Such results show that magnet coupling makes a big role of vibration isolation.

Acknowledgement

This work was supported by the Brain Korea 21 Project in 2002.

References

1. Fellows, C. J., "Permanent Magnet Couplings," CME, pp. 79 - 84, June 1979.
2. Yonnet, J. P., "A New Type of Permanent Magnet Coupling," IEEE Transactions on Magnetics, Vol. MAG-17, No. 6, November 1981.
3. Yonnet, J. P., "Permanent Magnetic Bearing and Couplings," IEEE Transactions on Magnetics, Vol. MAG-17, No. 1, January 1981.
4. Hornreich, R. M., and Shtrikman, S., "Opimal Design of Synchronous Torque Couplers," IEEE Transactions on Magnetics, Vol. MAG-14, No. 5, September 1978.
5. Kojima, H., and Nagaya, K., "Nonlinear Torsional Vibration of a Rotating Shaft System with a Magnet Coupling," Bulletin of JSME, Vol. 27, No. 228, June 1984.
6. Meirovitch, L., "Analytical Methods in Vibrations," Macmillan, 1967.
7. Weissmann, D., Proceedings of the 3rd International Workshop RE-Co Mag. Appl., Vol. 6, pp. 325, 1978.

8. Park, H., "A Study on the Vibrational Analysis of Rotating Shaft with Magnetic Coupling," Master Thesis, Seoul National University, 1992.
9. Kim, S. K., "A study on the Analysis of Dynamic Characteristics of Main Spindle Considering Nonlinear Characteristics of Bearing," Master Thesis, Seoul National University, 1988.
10. Harris, T. A., "Rolling Bearing Analysis," John Wiley and Sons, 1966.
11. Lee, Y. S., and Lee, J. W., "Modeling of misaligned rotor-ball bearing systems," Spring Conference Proceeding of the KSNVE, pp. 60-66, Pusan, Korea, May 1996.
12. Lee, Y. S., and Lee, J. W., "Vibration analysis of a misaliagned rotor system supported by ball bearings," Spring Conference Proceeding of the KSNVE, pp. 247-252, Kyoengju, Korea, May 1997.
13. Song, C. K, Sin, Y. J., and Lee, H. S., "Evaluation of performance of ultraprecision feeding system driven by the twist-roller friction drive," Fall Conference Proceeding of the KSPE, pp. 1170-1174, Korea, November 1998.
14. Cho, J. J., Kim, S. I., and Choi, D. B., "Dynamic characteristics analysis of main spindle built in motor," Fall Conference Proceeding of the KSPE, pp. 91-95, Korea, November 1993.